

Wear Simulation

Sören Andersson
Professor Emeritus in Machine Elements
Royal Institute of Technology (KTH), Stockholm,
Sweden

1. Introduction

1.1 Can the wear process be modelled and simulated?

The wear process can be modelled and simulated, with some restrictions. If we know the operating wear process, or how to model the wear process, we can also simulate and predict wear. In this presentation I will first outline how to use simplified estimations in machine design, and thereafter indicate how to perform more detailed wear simulations.

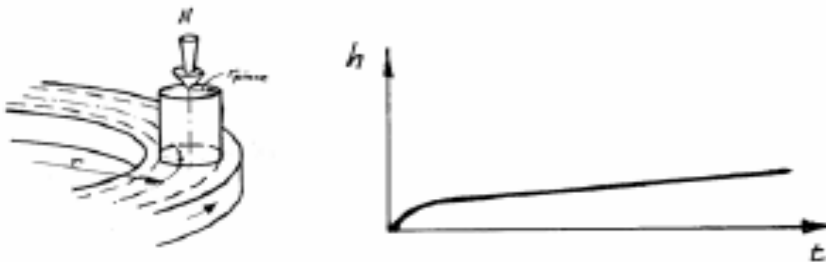


Fig. 1. Pin-on-disc test

Pin-on-disc experiments such as that shown in Figure 1 show that the wear is linearly proportional to the sliding distance, at least after a running-in period (a period that it can be difficult to measure, for a variety of reasons). Most wear models assume linearity, and they often also assume that the wear is directly proportional to the local contact pressure. The most common wear model is named Archard's Wear Law [1], although Holm [2] formulated the same model much earlier than Archard. However, Archard and Holm interpreted the model differently. The model has the following general form;

$$V = K \cdot \frac{F_N}{H} \cdot s, \quad (1)$$

where V is the wear volume, K is the dimensionless wear coefficient, F_N is the normal load, H is the hardness of the softer contact surface and s is the sliding distance. Equation (1) is often reformulated by dividing both sides by the apparent contact area A and by replacing K/H with k :

$$h = k \cdot p \cdot s \quad (2)$$

where h is the wear depth in m, k is the dimensional wear coefficient in m^2/N , p is the contact pressure in Pa and s is the sliding distance in m, as before. This wear model is widely used.

The wear coefficient is influenced by many factors, including whether the contact is mixed or boundary lubricated. Figure 2 shows how the dimensional wear coefficient depends on the lubricating conditions at the contact if the lubricant is clean. In many cases, however, the lubricant includes abrasive particles, which mean that even if the contact surfaces are well lubricated, they may become worn, as shown in figure 3. In such cases it is difficult to estimate the contact pressure, and so the wear assumption for abrasive contacts is often changed to state only that wear is proportional to sliding distance. The wear models in Figure. 3 are formulated as initial value wear models, as described later.

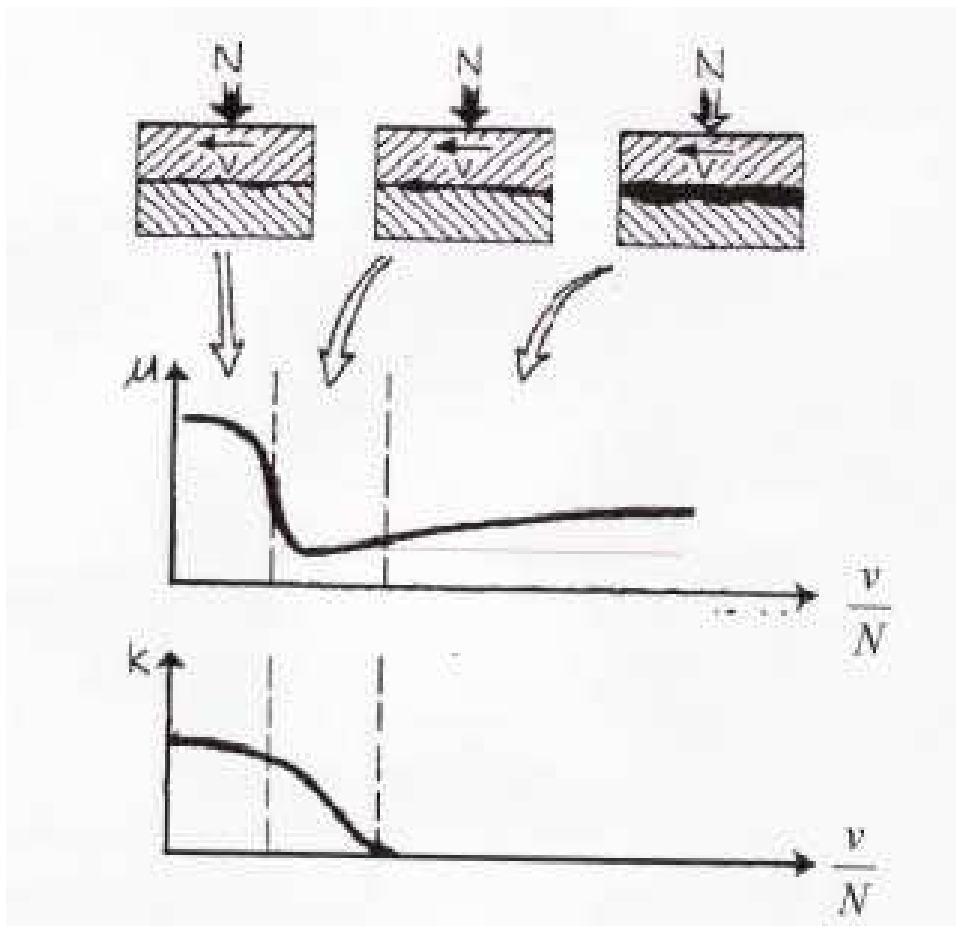


Fig. 2. The influence on the k-value of the lubrication conditions.

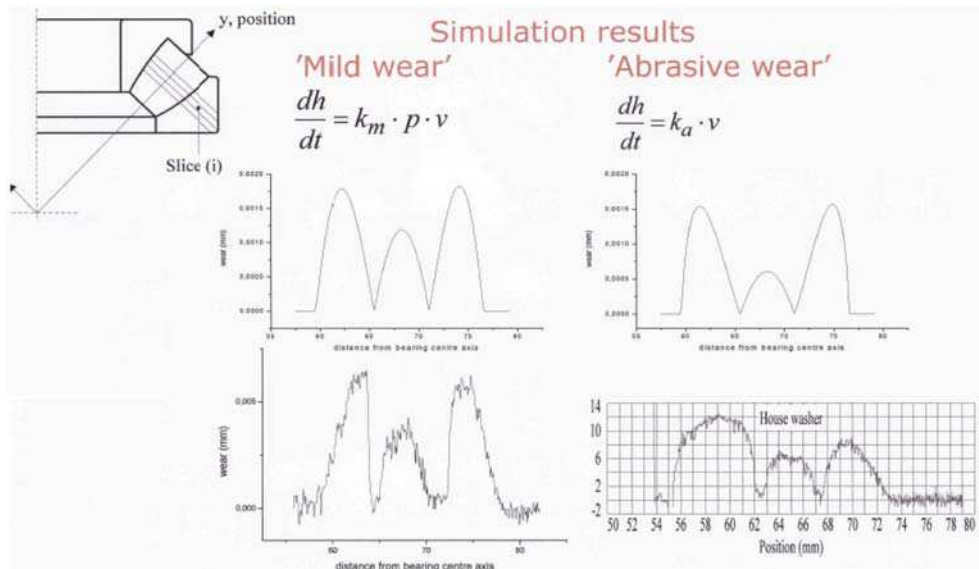


Fig. 3. Abrasive wear compared with mild sliding wear

The easiest and perhaps the most useful part of wear prediction is determining a good k value for a particular design. You can perform tests to determine this value, and compare the results with the estimated value. These estimates are based on the simple linear relation in equation (2) and involve a number of simplifications that vary from case to case. We also consult engineering handbooks and papers in international journals. Another way to approach this is by building up your own expert knowledge about typical k values based on previous estimates and experiments. This is what I have done for more than 10 years in industry. I have found that the best k value for dry contacts is about $1 \cdot 10^{-16} \text{ m}^2/\text{N}$. This value applies to a very smooth hard surface against a dry, filled Teflon liner. It is often necessary to lubricate contacts in order to obtain a reasonable operating life. For boundary-lubricated case hardening contact surfaces running under mild conditions, the value may be $1 \cdot 10^{-18} \text{ m}^2/\text{N}$. However, it is easy to get severe conditions in lubricated contacts, in which case the wear will increase about 100 times. In order to maintain mild conditions (i.e. to prevent transition to a severe situation), different types of nitrated surfaces are often used.

How can you ensure that the estimated k values are achieved in practice? Let's look at the example of a sliding journal bearing. You can perform a simple calculation of the k value needed to achieve a reasonably long operating life. If the value you calculate is between $1 \cdot 10^{-16} \text{ m}^2/\text{N}$ and $1 \cdot 10^{-18} \text{ m}^2/\text{N}$, you know that wear conditions must be mild, and that you need to lubricate the contact with a clean lubricant to keep them that way. If the answer is less than $1 \cdot 10^{-18} \text{ m}^2/\text{N}$, your task is challenging and you will need a separating film (full film lubrication) and a clean lubricant in order to be successful.

The approach I have just presented is a common way to predict whether a wear problem can be solved at the design stage, and is thus a very useful application of predictions or simulations. You can also carry out laboratory experiments to check your findings. However you should bear in mind that researchers often compare different materials and coatings

under harsh conditions, because mild wear takes too long to show. Consequently the results obtained are not very useful as a guide to wear under mild sliding conditions.

The above example shows you how it is possible to estimate wear during product development. This knowledge can be used to anticipate problems or design around them.

An expert in this field can usually suggest solutions to wear problems by doing simulations or estimations.

In the rest of this chapter, I will discuss more complex simulations and predictions of wear in high-performance machine elements.

2. Wear models and simulation methods

Wear can be defined as the removal of material from solid surfaces by mechanical action. Wear can appear in many ways, depending on the material of the interacting contact surfaces, the operating environment, and the running conditions. In engineering terms, wear is often classified as either mild or severe. Engineers strive for *mild wear*, which can be obtained by creating contact surfaces of appropriate form and topography. Choosing adequate materials and lubrication is necessary in order to obtain mild wear conditions. However, in order to get mild wear you often have to harden and lubricate the contacts in some way. Lubrication will often reduce wear, and give low friction. Mild wear results in smooth surfaces. *Severe wear* may occur sometimes, producing rough or scored surfaces which often will generate a rougher surface than the original surface. Severe wear can either be acceptable although rather extensive, but it can also be catastrophic which always is unacceptable. For example, severe wear may be found at the rail edges in curves on railways.

Mild and severe wear are distinguished in terms of the operating conditions, but different types of wear can be distinguished in terms of the fundamental wear mechanisms involved, such as adhesive wear, abrasive wear, corrosive wear, and surface fatigue wear.

Adhesive wear occurs due to adhesive interactions between rubbing surfaces. It can also be referred to as scuffing, scoring, seizure, and galling, due to the appearance of the worn surfaces. Adhesive wear is often associated with severe wear, but is probably also involved in mild wear.

Abrasive wear occurs when a hard surface or hard particles plough a series of grooves in a softer surface. The wear particles generated by adhesive or corrosive mechanisms are often hard and will act as abrasive particles, wearing the contact surfaces as they move through the contact.

Corrosive wear occurs when the contact surfaces chemically react with the environment and form reaction layers on their surfaces, layers that will be worn off by the mechanical action of the interacting contact surfaces. The mild wear of metals is often thought to be of the corrosive type. Another corrosive type of wear is fretting, which is due to small oscillating motions in contacts. Corrosive wear generates small sometimes flake-like wear particles, which may be hard and abrasive.

Surface fatigue wear, which can be found in rolling contacts, appears as pits or flakes on the contact surfaces; in such wear, the surfaces become fatigued due to repeated high contact stresses.

2.1 Wear models

Wear simulations normally exclude surface fatigue and only deal with sliding wear, even if it seems unlikely that the sliding component is the only active mechanism. Yet rolling and

sliding contacts are common in high performance machines. Thus the Machine Elements Department at KTH began to investigate whether sliding is actually the main source of wear in rolling and sliding contacts. We first studied this question in relation to gears, but have also simulated other contacts. In a rolling and sliding contact in a gear, the sliding distance per mesh is fairly short. The sliding distance of a contact point on a gear flank against the opposite flank is geometrically related to the different gear wheels and the load. In the first paper we published about wear in gears, we introduced what we called the 'single point observation method' [3] (explained in Fig. 5). We later found that this method is generally applicable, and have used it since then. You will now find the same principle being used under different names in other well-known papers, but we have chosen to stay with our original term.

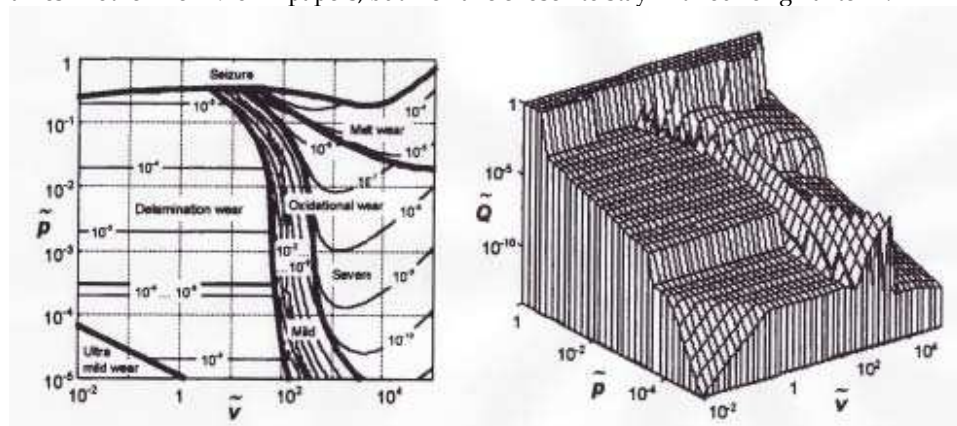


Fig. 4. a) Wear map according to Lim and Ashby [5] b) The same wear map according to Podra [20]

The possibility of predicting wear is often thought to be limited. Even so, many wear models [4] are found in the literature. These models are often simple ones describing a single friction and wear mechanism from a fundamental point of view, or empirical relationships fitted to particular test results. Most of them represent a mean value. The random characteristics of both friction and wear are seldom considered. In this chapter we present some of the models most used in simulations of wear in high performance machine elements.

Surfaces may wear if they rub against each other and are not completely separated by a clean oil film; they may also wear if the oil film separating them contains abrasive particles. The amount of wear is dependent on the properties of the surfaces, surface topography, and lubrication and running conditions. The best-known wear model is

$$\frac{V}{s} = K \frac{F_N}{H} \quad (3)$$

where V is the wear volume, s is the sliding distance, K is the dimensionless wear coefficient, H is the hardness of the softer contact surface, and F_N is the normal load. This model is often referred to as Archard's Wear Law [1].

By dividing both sides of equation (3) by the apparent contact area, A , and by replacing K/H with a dimensional wear coefficient, k , we get the following wear model:

$$\frac{h}{s} = k \cdot p \quad (4)$$

where h is the wear depth and p is the contact pressure.

Some scientists have tried to analyse the validity of the wear model according to equations (3) and (4), and one result of their work are wear maps or transition diagrams. The wear map of Lim and Ashby [5] (Fig. 4), shows two wear mechanisms: delamination wear and mild oxidational wear. Both these mechanisms are considered mild in engineering terms, and both produce thin, plate-like wear debris. Delamination wear theory, as developed by Suh [6], sets out to explain flake debris generation. Suh based his theory on the fact that there is a high density of dislocations beneath the contact surfaces. During sliding interactions between the contact surfaces, these dislocations form cracks that propagate parallel to the surfaces. The total wear volume is assumed to equal the sum of the wear volume of each contact surface. The basic wear model developed by Suh is:

$$V = N_1 \cdot (s/s_{01}) \cdot A_1 \cdot h_1 + N_2 \cdot (s/s_{02}) \cdot A_2 \cdot h_2 \quad (5)$$

where V is the wear volume, N_i is the number of wear sheets from surface i , A_i is the average area of each sheet, h_i is the thickness of the delaminated sheet, s_{0i} is the necessary sliding distance to generate sheets and s is the actual sliding distance. It is noticeable that the wear volume from each contact surface adds up the total wear volume, which was not clearly formulated before. Suh also stated that a certain sliding distance is required before a wear particle is formed. However, the sliding distance in his equation is equal for both surfaces, which indicates that he was not aware of the single point observation method.

Another interesting sliding wear mechanism is the oxidative wear mechanism proposed by Quinn [7], who stated that the interacting contact surfaces oxidize. The oxide layer will gradually grow until the thickness of the oxide film reaches a critical value, at which stage it will separate from the surface as wear debris. Even in this case a certain sliding distance is required before wear debris will be formed. Depending on whether the oxide growth is linear or parabolic, the wear is directly proportional to the sliding distance or to the power of the sliding distance. Experimental observations indicate that the wear is nearly directly proportional to the sliding distance under steady-state mild conditions.

Although Suh did not observe that the sliding distance points on the contact surfaces are different, the single point observation method has been found to be a very useful general method for understanding and modelling many friction and wear processes. This method was developed and successfully used in many projects at KTH Machine Design in Stockholm. The theoretical application of the method was based on formulas for the sliding distances in gears developed by Andersson [8]. He found that the distance traversed by a point on a gear flank against the opposing gear flank in one contact event varies depending on the position on the flank, the gear ratio, the size of the gears, and the loads applied to the gear tooth flanks. This finding about the sliding distance means that gear contacts cannot generally be replicated by rolling and sliding rollers. Simulations of the wear on gear flanks, based on sliding distance among other factors, has been validated by empirical measurements from gear tests. That observation and many years of pin-on-disc tests have inspired me and others to simulate friction and wear in rolling and sliding contacts of different types, and the results have been verified by experiments. This work has also improved our understanding of what occurs in contacts.

The single point observation method can be illustrated by the type of pin-on-disc experiment shown in Figure 1. A point on the pin contact surface is in contact all the time, but a contact point on the disc is only in contact with the pin when the pin passes that point. Even if the two contact surfaces have the same wear resistance, the pin will wear much more than the disc. Another illustration of the method is the two disc example shown in Fig. 5. The contact surfaces move with peripheral speeds of v_1 and v_2 , with $v_1 > v_2$. We observe a point on surface 1, P_1 , which has just entered the contact, and follow that point through the contact. We also note a point on surface 2, P_2 that is opposite the first observed point P_1 on surface 1 when it enters the contact. As P_1 moves through the contact, the interacting opposite surface will not move as fast as surface 1, since $v_1 > v_2$. A virtual distance $\Delta\delta_v = x \cdot (v_1 - v_2) / v_1$ in the tangential direction will occur between P_1 , the observed point, and a point P_2 . That distance is first compensated for by tangential elastic deformations of the contact surfaces $\Delta\delta_{el,1} + \Delta\delta_{el,2}$, but when that is no longer possible, the observed point will slide against the opposite surface for a distance $\Delta\delta_s$ equal to:

$$\Delta\delta_s = \Delta\delta_v - \Delta\delta_{el,1} - \Delta\delta_{el,2} \tag{5}$$

The frictional shear stress in the contact depends on the process, which means that at first it will be dependent mainly on elastic deformations. At higher torques or higher slip, the frictional shear stress will depend mainly on the sliding between the surfaces. Since these phenomena are always active in rolling and sliding contacts, it is interesting to analyse to what extent the stick zone, represented by the elastic deformation, influences the friction and wear in a contact. The results show that in many cases the effect of elastic deformation on friction and wear can be neglected.

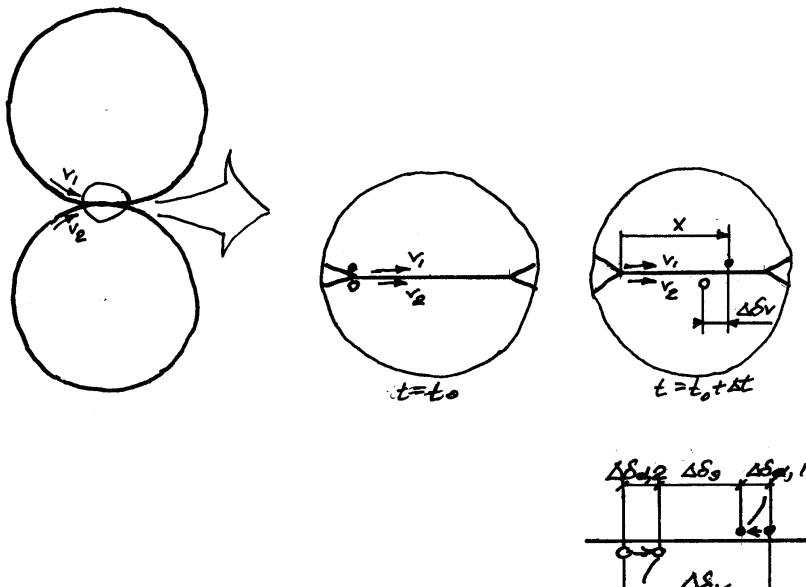


Fig. 5. Two discs: The basic principle for determining the sliding distance in a rolling and sliding contact

2.2 Wear maps and transition diagrams

As mentioned in the introduction, friction and wear can be of different types. It is thus helpful to know what types of friction and wear we can expect in a particular contact and when and why the transitions between different types occur. Some interesting research on that subject has been done, and continues to be done. I will briefly present some results from work on the transitions between different friction and wear modes. The relevant diagrams are often named wear maps or transition diagrams. The most referenced paper about wear maps is that by Lim and Ashby [5], (Fig. 4), who classified different wear mechanisms and corresponding wear models for dry sliding contacts. They studied the results of a large number of dry pin-on-disc experiments and developed a wear map, based on the parameters: $\tilde{Q} = \frac{V}{As}$, $\tilde{p} = \frac{F_N}{AH}$, and $\tilde{v} = \frac{vr_0}{a_0}$, where V is the wear volume, A is the apparent contact area, F_N is the normal load, H the hardness of the softer material in the contact, v the sliding velocity, r_0 the radius of the pin, and a_0 is the thermal diffusivity of the material.

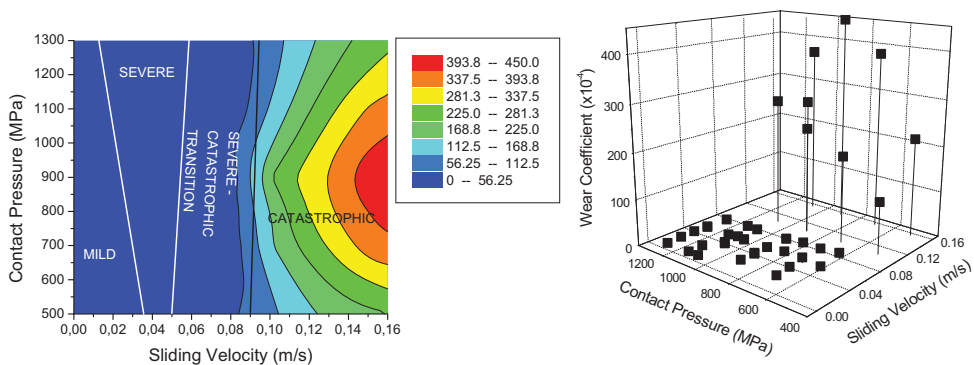


Fig. 6. Wear coefficient map according to Lewis and Olofsson [9].

Lewis and Olofsson [9] performed a similar investigation of contacts between railway wheels and tracks. Their goal was 'to produce tools in the form of maps of rail material wear data for identifying and displaying wear regimes and transitions'. They collected wear data from both laboratory and field tests, but found that data are often lacking for rail gauge and wheel flange contacts. They also collected available data and structured the data in different ways. Figure 6 shows an example of a wear coefficient map developed by Lewis and Olofsson [9]. The wear coefficient they used was determined using Archard's Wear Law. Sundh [10] has also done considerable work on transitions in wheel/rail contacts. His goal is to construct wear maps that include the contact between rail gauge and wheel flange. An additional goal is to study how the transitions from mild to severe wear depend on different types of lubricants, surface coatings and topographies. He studies both dry and lubricated contacts.

For lubricated contacts, the degree to which a lubricant separates the surfaces very strongly influences both the friction and the wear. The degree of separation is often divided into boundary lubrication, mixed lubrication, and full-film lubrication (Fig. 2).

Boundary lubrication refers to lubrication in which the load is supported by the interacting surface asperities and the lubrication effect is mainly determined by the boundary

properties of the lubricant between the interacting asperities. In *mixed lubrication*, the lubricant film itself supports some of the load in the contact, though the boundary properties of the lubricant are still important. In this case, the hydrodynamic and elastohydrodynamic effects are also important. Mixed lubrication is therefore sometimes referred to as partial lubrication or partial elastohydrodynamic lubrication (EHL). In *full-film lubrication*, the interacting contact surfaces are fully separated by a fluid film. In the literature, full-film lubrication is sometimes referred to as elastohydrodynamic lubrication, since the film-formation mechanism of high-performance contacts and local asperity contacts is probably elastohydrodynamic.

As mentioned in the introduction, transitioning from a desired mild situation to a severe situation should be avoided. Research has been performed to determine when and under what conditions transitions from one kind of friction and wear to another may occur in lubricated contacts. One such study developed what is called an IRG transition diagram [11] on which one can identify different lubrication regimes: a mixed or partial elastohydrodynamic lubrication regime, a boundary lubrication regime, and a failure regime. The last regime is sometimes called the scuffed or unlubricated regime and is a severe condition. The other regimes are mild.

The transition from a desired mild regime to a severe regime has also been studied by Andersson and Salas-Russo [12]. They used the track appearance as the transition criterion. When a significant part of the track is scored, seized or strongly plasticized, severe conditions are in effect. They found that for bearing steels the surface topography has a stronger influence on the mild to severe transition level than does the viscosity of the lubricant (Fig. 7). That was later confirmed by Dizdar [13].

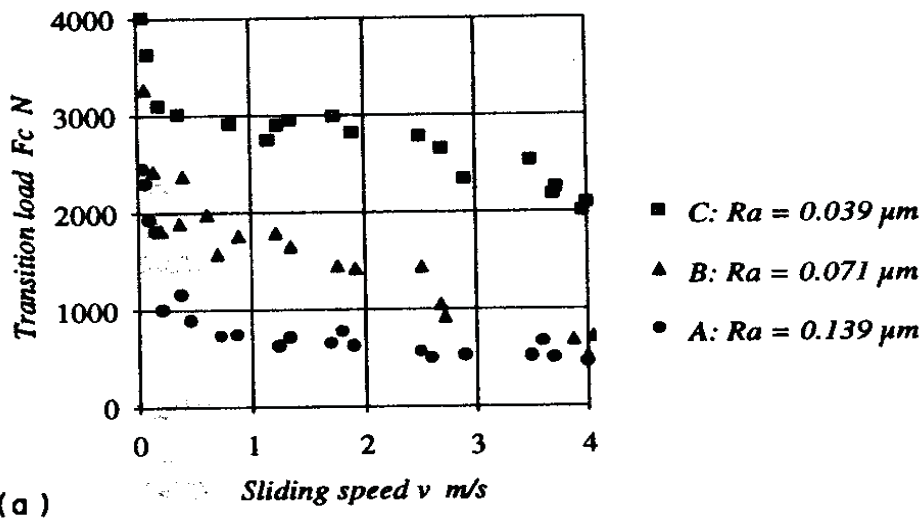


Fig. 7. The influence of surface roughness on the transition load of a lubricated sliding steel contact. Ball ($d=10$ mm) and disc material: SAE52100, $H_{v,ball} = 8000-8500$ MPa, $H_{v,disc} = 5800-6300$ MPa, $R_{a,ball} = 0.008\mu\text{m}$. Lubricant: ISO VG 46 mineral oil. [12]

The Machine Elements Groups at KTH in Stockholm and at the Luleå Technical University in Luleå, along with a number of Swedish companies, have pursued a research program

named INTERFACE. The goal of the program was to develop relevant friction and wear models for simulations in industry of different types of mechanical devices. The program was based on previous work by Sellgren [14], who developed general principles for modelling systems. His approach was modular, and laid down strict guidelines for behavioural models of machine elements, modules, and interfaces. Sellgren defined an interface as an attachment relation between two mating faces. That definition was elaborated on by Andersson and Sellgren [15] in terms of an interaction relation between two functional surfaces. A functional surface is a carrier of a function.

2.3 Sliding wear in a rolling and sliding contact

Predicting the amount of wear is generally thought to be rather difficult and uncertain. This section however addresses this task, outlining some possibilities for predicting wear in rolling and sliding contacts, and thus in the general case, the wear in most type of contacts. If the rolling and sliding contacts are running under boundary or mixed conditions, the wear of the contact surfaces is often low. If the surfaces are contaminated with particles, however, wear may be extensive. Different environmental contaminants may reduce or increase friction and wear, but they always have a strong influence on both.

In a rolling and sliding contact, the two interacting surfaces characteristically move at different speeds in a tangential direction. The Tribology Group at KTH Machine Design has performed simulations of friction and wear in rolling and sliding contacts for a long time. The modelling principles the group has successfully used are based on 1) the single-point observation method and 2) treating wear as an initial-value process.

Wear in rolling and sliding contacts can be of different types. If a surface is subject to high, repeated dynamic loading, surface fatigue may occur, and pits may form on the surface. Here, however, we will not deal with surface fatigue; instead, we will focus our attention on sliding wear. To illustrate the wear process, a typical wear curve obtained in a pin-on-disc testing machine using a flat-ended cylindrical pin rubbing against a disc under any condition is shown in Figure 8.

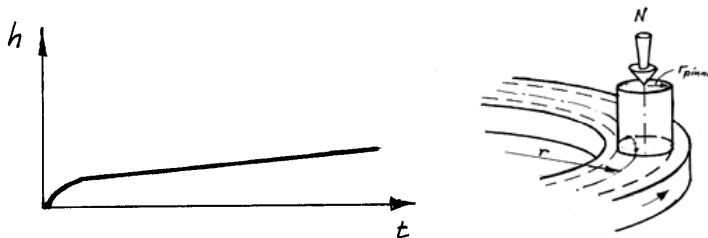


Fig. 8. A schematic wear curve from a pin-on-disc test with a flat ended cylindrical pin

A typical wear process always starts with a short running-in period during which the highest asperities and the contact surfaces in general are plastically deformed and worn; this is followed by a steady-state period in which the wear depth is directly proportional to the sliding distance. The initial running-in period is rather brief but not very well understood.

The general appearance of a wear curve seems to be similar for dry, boundary and mixed lubricated contacts, as well as for contacts with lubricants contaminated with abrasive particles. Aside from ease of testing, the pin-on-disc configuration is a popular testing geometry because most of the wear is on the pin. The distance a point on the pin's contact

surface slides against the disc is much longer than the corresponding distance a contact point on the disc slides against the pin during a single revolution of the disc.

Simple pin-on-disc test results indicate that sliding distance is an important parameter determining sliding wear. For rolling and sliding contacts, the sliding part of the surface interactions, although not obvious, is therefore of interest. Some researchers maintain that the effect of sliding is negligible in most rolling and sliding contacts. Various investigations have demonstrated, however, that the distances the contacts slide against the opposite interacting surfaces during a mesh are sufficient to form wear debris in most rolling and sliding contacts. For this reason, we will show how much a point on a contact surface slides against an opposite contact surface during a mesh.

Consider two discs that are pressed together and run at different peripheral velocities (see Fig. 5 above). This is a typical situation in tractive rolling contacts. The absolute value of the sliding distance is s_i , with $i = 1$ a point on the contact surface of body 1 and $i = 2$ a point on the contact surface of body 2. The sliding distance, s_i , during one mesh at a point on one of the contact surfaces sliding against the opposite interacting surface is equal to

$$s_i = 2a \cdot \left| \frac{v_1 - v_2}{v_i} \right| \quad (6)$$

where a is the half width of the contact, v_1 is the peripheral velocity of surface 1, and v_2 is the peripheral velocity of surface 2. The sliding distances in rolling and sliding contact according to Equation (6) apply to rollers.

For contacts between other bodies, such as gears and railway wheels and rails, determining the sliding distances may be more complicated. The principle, however, is the same, namely, to study the distance a point on a contact surface slides against the opposite surface during a single mesh.

In the examples shown, the elastic deformations of the contact surfaces in the tangential direction are ignored; those displacements would reduce the sliding distance a little, but micro-displacements normally have very little effect on the contact conditions.

2.4 Wear simulation

The single point observation method was initially found to be very useful during our work on simulating friction and wear of boundary-lubricated spur gears [3] as previously mentioned (Fig. 9). The distance a point on a gear flank slides against an opposite flank during one mesh varies depending on the position on the flank, the gear ratio, the size of the gears, and the loads applied on the gear tooth flanks. The principle for determining these sliding distances is shown in Fig. 9. In this figure the sliding distance is referred to as g , although s is used elsewhere in this paper.

Test results obtained indicate that the amount of wear on the gear flanks seems to correlate with the sliding distances recorded. That observation and many years of pin-on-disc tests have inspired us to try to simulate sliding wear in rolling and sliding contacts. Our first effort was a simulation of the mild wear of gear tooth flanks under boundary-lubricated conditions [3] (Fig. 10). The first wear simulation was based on the wear model shown in Equation (4). The simulation was simplified by assuming that the wear coefficient was constant throughout the process, and the initial running-in period was not considered. The contact pressure between the flanks was assumed to be constant (i.e., the mean contact

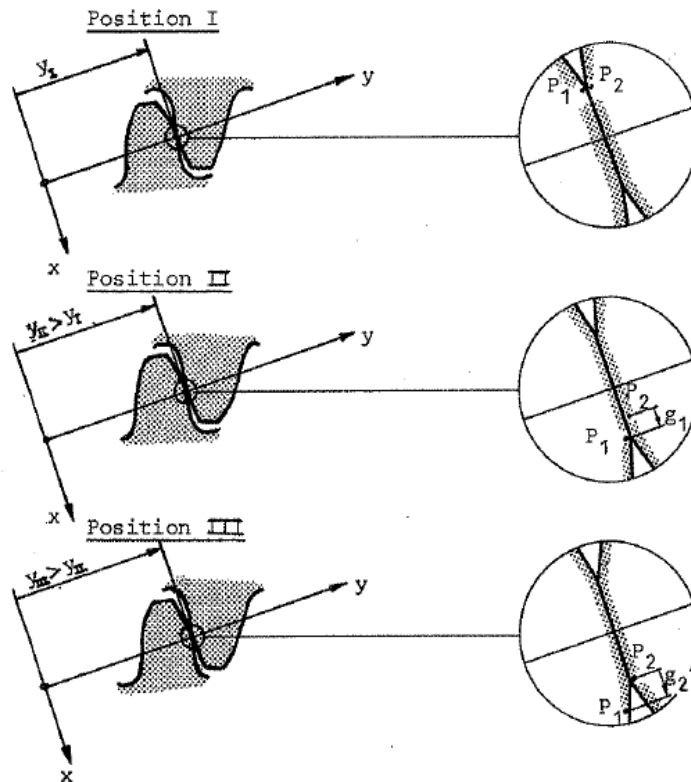


Fig. 9. The distance, g_1 , point P_1 on the pinion flank and the distance, g_2 , point P_2 on the gear flank slide during one mesh; position I corresponds to the moment in time when P_1 and P_2 come into contact with each other, while positions II and III correspond to the moments in time when P_1 and P_2 disengage, respectively. [8]

pressure was determined and used). This assumption is acceptable as long as the wear model is linear. Using these simplifications and the sliding distances determined according to derived equations, it was possible to simulate the wear depth at a particular point on a gear flank (the wear simulation was run as a simple spreadsheet program). The wear distribution and estimated wear coefficient were found to be in reasonably good agreement with the experimental observations. Our awareness of the risk that the basic principle and simplifications used in the model might only be relevant to this particular case motivated us to continue our research into simulating wear in rolling and sliding contacts. Further studies were successfully conducted to determine how generally applicable the principle and the simplifications are.

The principle when modelling the process is to start with the wear model, which is best formulated as a first order differential equation with respect to time, as shown below. If we use Euler's method to numerically integrate the equation, we have to determine the parameters for sliding speed and local contact pressure for all points on the contact surfaces at each time step. Determining the parameters is often rather time-consuming, and thus the integration and simulation also take time.

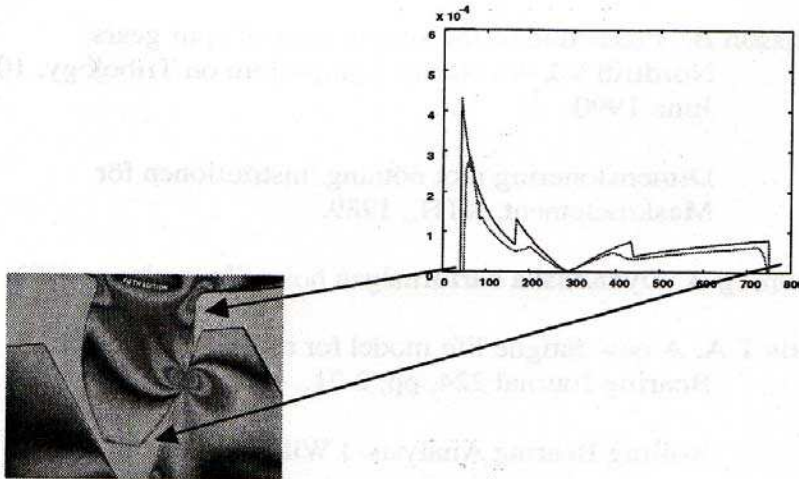


Fig. 10. Results of two simulations of a spur pinion. The sharp curves are from Andersson and Eriksson [3] and the other is from Flodin [18].

2.5 Wear as an initial-value process

Wear is seldom a steady-state process, even if steady-state conditions are desirable and often predominate in the wear process. Normally, the running-in wear is greater than the ensuing wear. The forms of the contact surfaces are often such that the wear depth will vary with time. Moreover, mild wear of the contact surfaces causes geometric changes that initiate other wear processes. Olofsson [16], for example, found that mild wear of the contact surfaces of spherical thrust roller bearings increases the contact pressure at the pure rolling points. The increased contact pressure means that surface fatigue wear at the pure rolling points begins much earlier than expected.

As a direct result of that finding, and because wear simulations often contain many simplifications, we started to investigate wear simulations from a mathematical-numerical point of view. We found that simulations of wear processes can be regarded as initial-value problems [17]. We know the initial conditions and properties of the contacts fairly well, and if we can also formulate how the surfaces change, it should be possible to predict the states of the surfaces at any time during operation. The wear rate may then be formulated according to the following model:

$$\frac{dh}{dt} = f(\text{material, topography, lubricant, load, velocity, temperature,}) \quad (7)$$

where h is the wear depth at a particular point on an interacting surface and t is time. This formulation is in agreement with the dynamic behaviour of mechanical systems and can easily be numerically integrated. A model often used in many wear simulations is

$$\frac{dh}{dt} = k \cdot p \cdot v_s \quad (8)$$

where v_s is the sliding velocity. The wear model in Equation (8) may be regarded as a generalization of Archard's wear law (see Eq. (3) and (4)).

Equation (8) is often reformulated as:

$$\frac{dh}{ds} = k \cdot p \quad (9)$$

since $ds = v_s dt$ is often true.

2.6 Determination of the pressure distribution

When working with the linear relation between wear, pressure and sliding distance, the determination of the contact pressure at a particular point is often the trickiest and most time-consuming part of the simulation. The deformation at a particular point is dependent on the deformation of all other points around the observed point, which implies a rather complex process for accurately calculating the pressure distribution. Today, there are several different approaches to determining the contact pressure.

Finite element (FE) calculation is becoming increasingly popular as computer power increases and FE programs improve. The main drawback of the FE method is that determining the pressure distribution often entails considering a great many small elements on the surfaces. This is often difficult to do, since the combination with the body models often leads to a huge number of elements and a very long calculation time. The FE method will probably be used more in the future for interface-related problems than it is today.

Boundary element (BE) methods are commonly used to determine the micro-topography in the contact zone. BE programs are often based on the same assumptions that Hertz used when he derived his equations. As a result, most BE programs cannot be used for all applications. The BE method becomes a numerical process that is solved in different ways in order to obtain a reasonably accurate result as quickly as possible [20,21]. Some smart combinations of BE and FE methods will probably be used in future.

Machine Elements in Luleå are using another very promising method to determine the contact deformation and the pressure distribution.

A common way to simplify the determination of local pressure is to use a Winkler surface model in which the surfaces are replaced by a set of elastic bars, the shear between the bars is neglected, and the contact pressure at a point depends only on the deformation at that point according to

$$p = K_N \cdot u_z \quad (10)$$

where u_z is the deformation of the elastic rod. The spring constant, K_N , can be determined by

$$K_N = C_w \cdot \frac{E'}{b} \quad (11)$$

where $C_w \approx 1$, E' is the combined elastic modulus of the contact surfaces, and b is approximately the width of the elastic half space according to Hertz. The Brush model is an extension of the Winkler model to take tangential deformations into account. The Brush model is often used for simulating friction in complex contacts.

The Winkler method cannot be used for local phenomena, but some reasonable results can be obtained for complete contacts.

2.7 Numerical integration of a wear model

Equation (8) is a commonly used in wear simulation. Numerically integrating a wear model entails discretising geometry and time. The simplest numerical integration method is the Euler method. The wear depth at a chosen point on a contact surface is determined by

$$h_{i,new} = h_{i,old} + k_i \cdot p_i \cdot |v_1 - v_2| \cdot \Delta t \quad (12)$$

where $h_{i,new}$ is the obtained wear depth on surface i , $h_{i,old}$ is the wear depth on i in the previous simulation loop, k_i is the dimensional wear coefficient multiplied by the number of meshes or revolutions before geometry is changed, p_i is the local pressure at i when the actual time step starts, and Δt is the time step. Other numerical integration methods can, of course, be used in similar fashion, as different schemes are used in behavioural simulations of dynamic technical systems.

After a simulation, one must always check its accuracy. Common tests for doing so are the k and Δt checks. However, if the values chosen for these are too large, the results may not be correct. A common way to handle this is to check whether the same results are obtained using half the values of k or Δt .

One of the most difficult and time-consuming parts of a simulation is determining the pressure at a particular point in each simulation loop because pressure at any point depends on the pressure at all other points in the contact.

3. Typical results and their applicability (KTH)

At the start of this chapter, I demonstrated a simple method of estimating wear for a new designs, and I have also dealt with the typical k values for dry and boundary lubricated journal bearings. It is very important that anyone working in the field of tribology be able to make such estimates and understand their implications for the engineering design process.

At this point I will present some results of more accurate simulations of wear and their applicability. As previously mentioned, simulation of wear at KTH began with the simulation of mild wear in gears [3]. The process was programmed using a spreadsheet, since many simplifications were used. Later more accurate simulations of wear in gears were conducted by Flodin [18]. Figure 10 shows a comparison of the results obtained using the two methods to analyse wear in spur gears. Flodin also conducted experiments to correlate theoretical results with experimental results.

Not long after the initial gear wear simulation, a very difficult simulation of wear at the contact between a cam and a follower was performed by Hugnell et al. [19]. The contact is a rolling and sliding contact between the cam and the follower, which is rotating at the same time as it is moving. The result of a simulation is shown in Fig. 11.

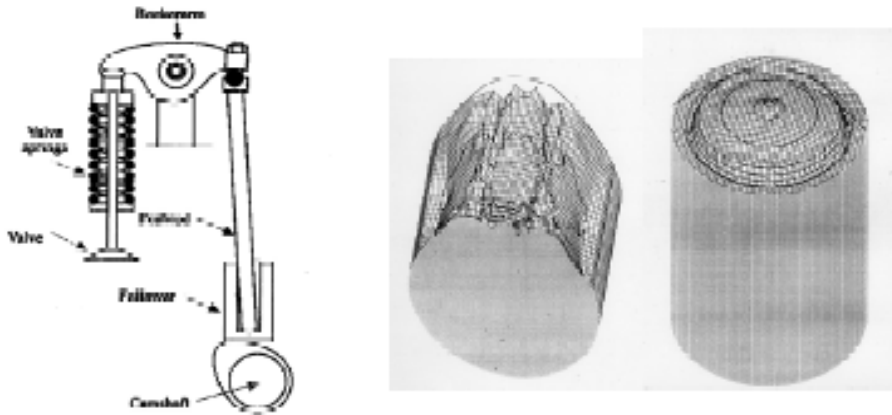


Fig. 11. Result of a wear simulation by Hugnell et al. [19]

3.1 Determining the wear of interacting rollers

We consider two cylindrical rollers both of radius R . The rollers are pressed together by force F_N and rotate at angular velocities ω_1 and ω_2 , respectively. The peripheral velocities of the contact surfaces are $v_1 = \omega_1 \cdot R$ and $v_2 = \omega_2 \cdot R$. The wear of the contact surfaces is assumed to be properly described by the following wear model:

$$\frac{dh_i}{dt} = k_i \cdot p \cdot v_{s,i}$$

where $i=1$ for roller 1 and $i=2$ for roller 2; h_i is the wear depth at a point on surface i when it rubs against the opposite contact surface, k_i is the wear coefficient for a point on surface i when it rubs against the opposite contact surface, p is the local contact pressure, and $v_{s,i}$ is the sliding velocity at a point on surface i sliding against the opposite interacting surface. The sliding velocity, $v_{s,i}$, for points on both contact surfaces equals

$$v_{s,i} = |v_1 - v_2|$$

We assume that the rollers are subject to a constant load and that the angular velocities are constant. The wear model will then have the following form after integration:

$$\int_0^{h_i} dh_i = k_i \cdot |v_1 - v_2| \int_0^t p dt$$

$$h_i = k_i \cdot |v_1 - v_2| \cdot \int_0^t p dt$$

If we study complete meshes, the contact pressure, p , can be replaced by the mean contact pressure, p_m . The wear depth is small compared with the radius of the rollers; p_m can thus

be determined once and used for all simulated revolutions. The integral equation can thus be reformulated according as follows:

$$h_{i_{new}} = h_{i_{old}} + k_i \cdot p_m \cdot |v_1 - v_2| \cdot \Delta t$$

If Δt is very small, so that only one point on each of the contact surfaces passes the contact once, then the wear of each surface per mesh will be

$$h_{1/mesh} = k_1 \cdot p_m \cdot \frac{|v_1 - v_2|}{v_1} \cdot 2a$$

and

$$h_{2/mesh} = k_2 \cdot p_m \cdot \frac{|v_1 - v_2|}{v_2} \cdot 2a$$

respectively.

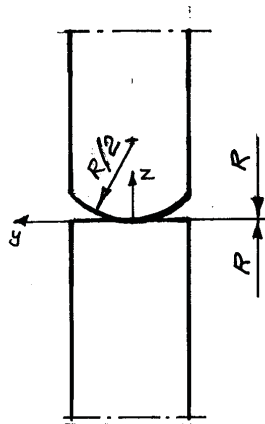


Fig. 12. Interacting modified roller and cylindrical roller

If surface 1 is moving faster than surface 2, in the long run points on surface 1 will be in contact more often than points on surface 2. Consequently, the wear of the two surfaces will only differ in relation to the wear coefficients. This can be demonstrated by the following relationships: Assume that the mechanism has been running for a fairly long time and that roller 1 has rotated n_1 revolutions. Roller 2 has then rotated $n_2 = n_1 \cdot (\omega_2 / \omega_1)$ revolutions. The wear of the rollers will then be as follows:

$$h_{1/longtime} = k_1 \cdot p_m \cdot \frac{|v_1 - v_2|}{v_1} \cdot 2a \cdot n_1$$

$$h_{2/longtime} = k_2 \cdot p_m \cdot \frac{|v_1 - v_2|}{v_2} \cdot 2a \cdot n_2 = k_2 \cdot p_m \cdot \frac{|v_1 - v_2|}{v_2} \cdot 2a \cdot \frac{\omega_2}{\omega_1} \cdot n_1 = k_2 \cdot p_m \cdot \frac{|v_1 - v_2|}{v_1} \cdot 2a \cdot n_1$$

since $v_1 = \omega_1 \cdot R$ and $v_2 = \omega_2 \cdot R$.

From an experimental point of view, it is advantageous to change the form of roller 1 so that the contact surface will have a radius of $R/2$ perpendicular to the direction of motion of the

contact surface (Fig. 12). The contact will then be a point contact instead of a line contact as in the previous example. This change improves the experimental set-up, but unfortunately it makes the wear simulation more difficult. The assumption that the wear coefficients for points on each surface are constant throughout the whole process is, however, relevant even in this case. The sliding velocity can also be assumed to be constant. As in the previous example, the contact pressure variation at a point on a surface during a mesh can be replaced by a mean pressure. An important difference, however, is that the mean pressure does not remain constant throughout the whole wear process, since the wear of the contact surfaces will change the pressure distribution in the contact. We assume that the same wear model as in the previous example is valid in this case as well. The resulting equation, after considering the simplifications, will be as follows:

$$h_{i,new} - h_{i,old} = k_i \cdot p_m \cdot |v_1 - v_2| \cdot (t_{new} - t_{old})$$

When the contact surfaces wear, the forms of the surfaces will change and thus also the pressure distribution in the contact. This means that we cannot assume that the pressure is constant, so we cannot, as in the previous example, run a large number of revolutions in one simulation loop. Thus there are two questions in this case: determining the local pressure at a point in every simulation loop, and deciding on the duration of each loop before a new local pressure determination must be made.

In this case, we do not have a standard Hertzian contact case, so we make b equal to the radius of a contact cylinder between the sphere of radius $R/2$ against a plane. A Winkler surface model of rod stiffness K_N is used to simulate the wear process of a modified roller interacting with a cylindrical roller. The contact surfaces are divided into a number of slices of width $\Delta y = b/10$ perpendicular to the sliding direction (Fig. 13). We assume that we can simplify the wear simulation by determining the wear for each slice in the same way as before. The penetration, d , of the modified upper roller against the lower cylindrical roller is determined so that the sum of the load of each slice support equals the applied force, F_N . The local wear can now be determined and the geometry of the contact surfaces modified. Thereafter, a new penetration, d , is determined, and so on. Figure 14 presents some simulation results for a modified upper roller interacting with a cylindrical roller. The rollers will wear while running. The wear of the discs will increase in both depth and width with time (see Fig. 14).

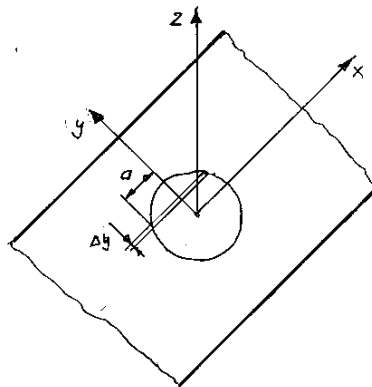


Fig. 13. Contact point and coordinate system, sliced contact

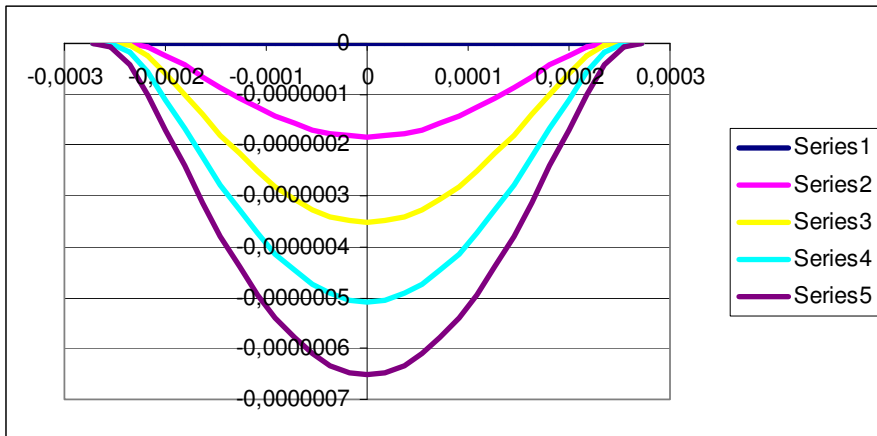


Fig. 14. Simulated wear of an ellipsoidal roller 1 interacting with a cylindrical roller 2. $R_{1x} = 25 \cdot 10^{-3} \text{ m}$, $R_{1y} = 12.5 \cdot 10^{-3} \text{ m}$, $R_{2x} = 25 \cdot 10^{-3} \text{ m}$, $F_N = 100 \text{ N}$, $v_1 = 1.25 \text{ m/s}$, $v_1 - v_2 = 0.06 \text{ m/s}$. Series 1 is at $t=0$, Series 2 is after n revolutions, Series 3 is after $2n$ rev., Series 4 is after $3n$ rev. and series 5 is after $4n$ rev.. The figure shows the change in shape of the contact surface of the rollers during running.

3.2 Concluding remarks

The wear of rolling and sliding contacts can be simulated. The basic principles to be remembered are 1) use the single point observation method and 2) treat the wear process as an initial-value problem. Using these principles, nearly any practical case can be simulated if you have a relevant wear model that can imitate the behaviour of a particular case. The most common wear model is the one known as Archard's generalized wear model:

$$\frac{dh}{dt} = k \cdot p \cdot v_s$$

How well that model describes the wear process is still being investigated. In many cases, however, simulated wear distributions agree fairly well with experimental observations. Wear simulations are quite often done stepwise, with repeated determinations of pressure, sliding velocities, etc. Determining the pressure distribution in the contact is often considered the most difficult and time-consuming task, and thus much effort is put into the task. Most simulations are done numerically, so choosing the appropriate surface element size and time step is critical. Too long a time step may produce incorrect results or an unstable simulation, while too short a time step, on the other hand, may result in excessive computation time. I believe that the main research tasks in the near future will be to develop relevant wear models accommodating transitions and choice of time step size, and the determination of pressure distributions.

3.3 Some examples from KTH

The three examples shown previously are results from the author and Hugnell et al. [19]. Flodin [18] results from the author, Hugnell et al. [19] and Flodin [18]. Figure 15 shows some of the results obtained by Flodin [18]. Figure 15 shows some of the results obtained.

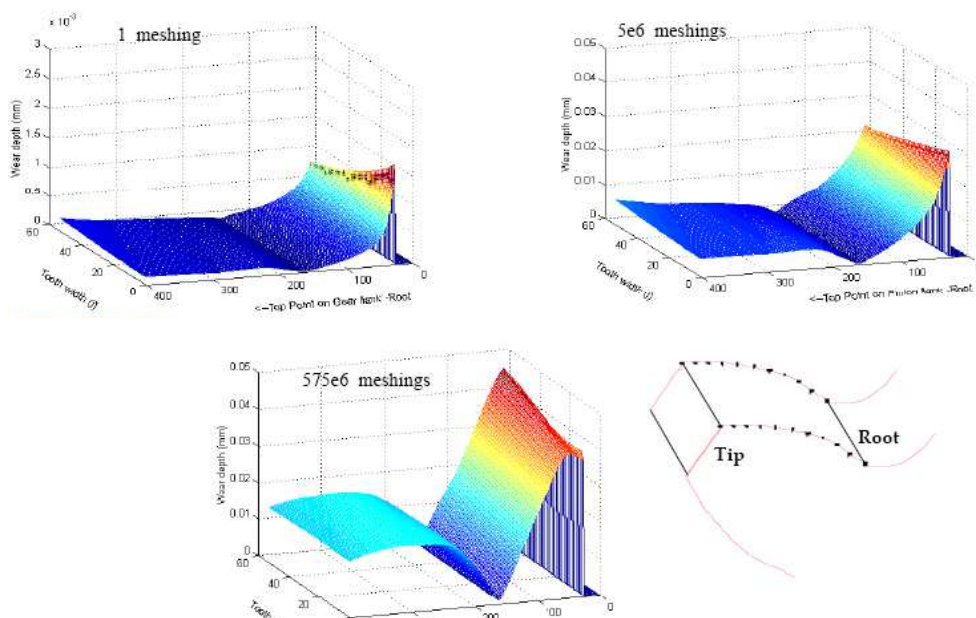


Fig. 15. Wear simulation results obtained by Flodin [18]

The programs Flodin developed were used by MacAldener [21] in his investigation of the influence of wear on judgements of the manufacturing robustness of gears.

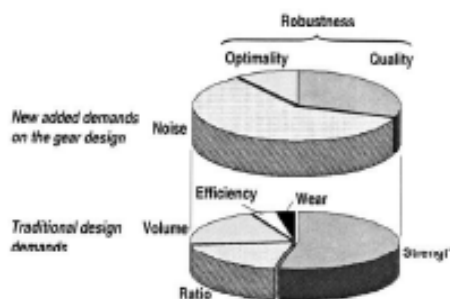


Fig. 16. The demands on a new gear developer and manufacturer [21]

Spiegelberg [23] performed some wear simulations of a rolling and sliding contact in an engine mechanism. His results can be used in different ways depending on the running conditions in the contact.

Another interesting application of work done at KTH is that of Åkerblom [22] who used the knowledge developed within the INTERFACE project. He found that the preset loading of bearings strongly influences noise excitation from a gearbox. The influence seems to be stronger than the effect of transmission error.

Podra [20] performed the first FE wear simulation. Söderberg [24] recently simulated wear in disc brakes using FE.

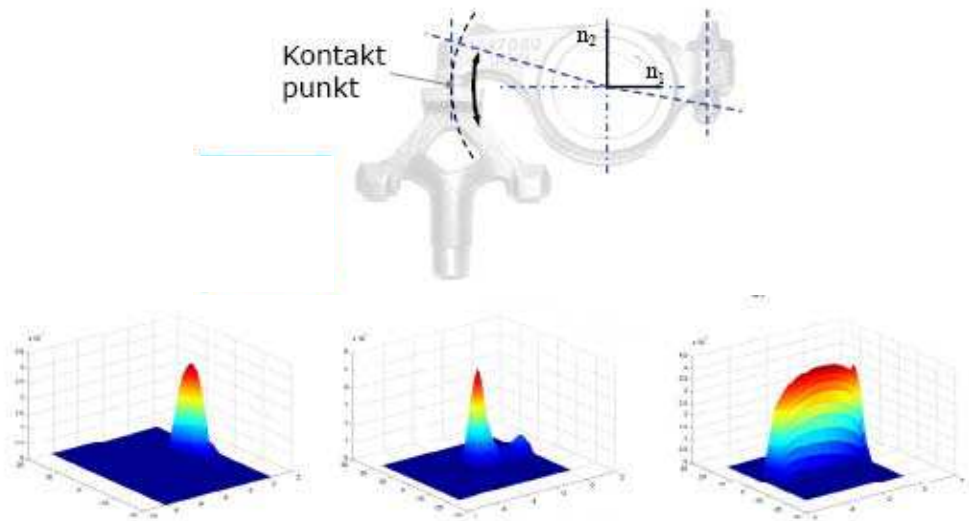


Fig. 17. Some wear simulation results obtained by Spiegelberg [23]

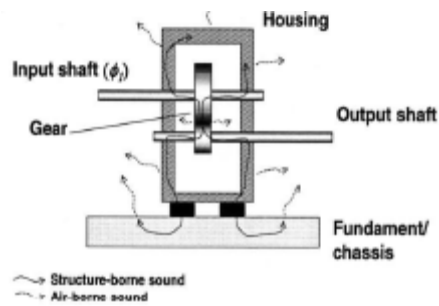


Fig. 18. Noise excitation from a gearbox [22]

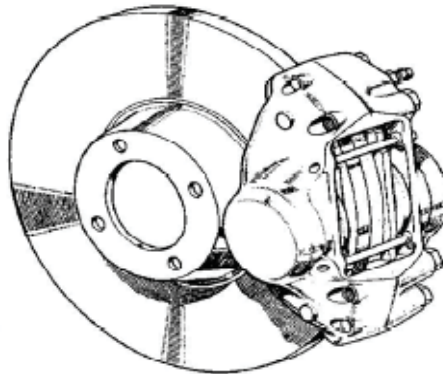


Fig. 19. The disc brake subjected to wear simulations by Söderberg [24]

4. References

- [1] Archard, J.F. (1980) Wear theory and mechanisms. In: M.B. Peterson, W.O. Winer (eds.). *Wear Control Handbook*. ASME.
- [2] Holm, R. (1946) *Electric Contacts*. Almqvist & Wiksells Boktryckeri AB, Uppsala.
- [3] Andersson, S. and Eriksson, B. (1990) Prediction of the sliding wear of spur gears. *Nordtrib'90*, Hirtshals, Denmark.
- [4] Meng, H.-C. (1994) Wear modeling: Evaluation and categorization of wear. Dissertation, University of Michigan.
- [5] Lim, S.C. and Ashby, M.F. (1987) Wear mechanism maps. *Acta Metal.*, 35(1), pp. 1-24.
- [6] Suh, N.P. (1973) The delamination theory of wear, *Wear*, 25, pp. 111-124.
- [7] Quinn, T.F.J. (1962) Role of oxidation in the mild wear of steel. *British Journal of Applied Physics*, 13, pp. 33-37.
- [8] Andersson, S. (1975) Partial EHD theory and initial wear of gears. Doctoral thesis, Department of Machine Elements, KTH, Stockholm, Sweden.
- [9] Lewis R. and Olofsson, U. (2004) Mapping rail wear regimes and transitions. *Wear*, 257, pp. 721-729.
- [10] Sundh, J. (2009) On wear transformations in the wheel-rail contact. Doctoral thesis, Dept. of Machine Design, KTH.
- [11] Begelinger, A. and DeGee, A.W.J. (1981) Failure of thin film lubrication. *ASME J. Lubrication Techn.*, 103.
- [12] Andersson, S. and Salas-Russo, E. (1994) The influence of surface roughness and oil viscosity on the transition in mixed lubricated sliding contacts. *Wear*, 174, pp. 71-79.
- [13] Dizdar, S. (1999) Formation and failure of chemireacted boundary layers in lubricated steel contacts. Doctoral thesis. Dept. of Machine Design, KTH.
- [14] Sellgren, U. (2003). Architecting models of technical systems for non-routine simulations. International Conference on Engineering Design, ICED 03, Stockholm, August 19-21.
- [15] Andersson, S. and Sellgren, U. (2004) Representation and use of functional surfaces. 7th Workshop on Product Structuring-Product Platform Development, Chalmers University of Technology, Gothenburg, March 24-25.
- [16] Olofsson, U. (1997) Characterisation of wear in boundary lubricated spherical roller thrust bearings, *Wear*, 208, pp. 194-203.
- [17] Strang, G. (1986) *Introduction to Applied Mathematics*. Wellesley-Cambridge Press. ISBN 0-9614088-0-4.
- [18] Flodin, A. (2000) Wear of spur and helical gears. Doctoral thesis, Dept of Machine Design, KTH.
- [19] Hugnell, A., Björklund, S. and Andersson, S. (1996) Simulation of the mild wear in a cam-follower contact with follower rotation. *Wear*, 199, pp. 202-210.
- [20] Podra, P. (1997) FE wear simulation of sliding contacts. Doctoral thesis, Dept. of Machine Design, KTH.
- [21] MacAldener, M. (2001) Tooth interior fatigue fracture and robustness of gears. Doctoral thesis, Dept. of Machine Design, KTH.
- [22] Åkerblom, M. (2008) Gearbox noise. Doctoral thesis, Dept. of Machine Design, KTH.
- [23] Spiegelberg, C. (2005) Friction and wear in rolling and sliding contacts. Doctoral thesis, Dept. of Machine Design, KTH.
- [24] Söderberg, A. (2009) Interface modelling: friction and wear. Doctoral thesis, Dept. of Machine Design, KTH.



Advanced Knowledge Application in Practice

Edited by Igor Fuerstner

ISBN 978-953-307-141-1

Hard cover, 378 pages

Publisher Sciyo

Published online 02, November, 2010

Published in print edition November, 2010

The integration and interdependency of the world economy leads towards the creation of a global market that offers more opportunities, but is also more complex and competitive than ever before. Therefore widespread research activity is necessary if one is to remain successful on the market. This book is the result of research and development activities from a number of researchers worldwide, covering concrete fields of research.

How to reference

In order to correctly reference this scholarly work, feel free to copy and paste the following:

Sören Andersson (2010). Wear Simulation, Advanced Knowledge Application in Practice, Igor Fuerstner (Ed.), ISBN: 978-953-307-141-1, InTech, Available from: <http://www.intechopen.com/books/advanced-knowledge-application-in-practice/wear-simulation>

INTECH

open science | open minds

InTech Europe

University Campus STeP Ri
Slavka Krautzeka 83/A
51000 Rijeka, Croatia
Phone: +385 (51) 770 447
Fax: +385 (51) 686 166
www.intechopen.com

InTech China

Unit 405, Office Block, Hotel Equatorial Shanghai
No.65, Yan An Road (West), Shanghai, 200040, China
中国上海市延安西路65号上海国际贵都大饭店办公楼405单元
Phone: +86-21-62489820
Fax: +86-21-62489821

© 2010 The Author(s). Licensee IntechOpen. This chapter is distributed under the terms of the [Creative Commons Attribution-NonCommercial-ShareAlike-3.0 License](#), which permits use, distribution and reproduction for non-commercial purposes, provided the original is properly cited and derivative works building on this content are distributed under the same license.